Preparation of model catalysts by laser interference nanolithography followed by metal cluster deposition

M. Schildenberger [a], Y. Bonetti [b], M. Aeschlimann [a,*], L. Scandella [b], J. Gobrecht [b] and R. Prins [a]

[a] *Laboratory for Technical Chemistry, Federal Institute of Technology (ETH), 8092 Zurich, Switzerland*
[b] *Laboratory for Micro- and Nanostructures, Paul Scherrer Institute (PSI), 5232 Villigen, Switzerland*

Received 14 August 1998; accepted 29 September 1998

Metal clusters arranged on nanostructured oxidized silicon wafers are presented as new model catalyst systems. A photoresist layer spun on top of a wafer was patterned by laser interference exposure. The grid obtained after removing the exposed parts of the resist is used as an etching mask. Hollows with diameters of 300 nm and depths between 50 and 60 nm were etched into the oxide layer using wet chemical methods. Two methods were applied to deposit metal clusters (Pd or Cu) in a defined way within the hollows. The particles ranged from 10 to 50 nm in height and from 80 to 200 nm in diameter. The model catalyst systems were characterized by atomic force microscopy and X-ray photoelectron spectroscopy. The method presented here allows us to produce 4 inch wafers that are covered completely by nanometer-sized structures in a reasonable period of time.

Keywords: nanolithography, model catalyst, palladium, copper, stability, spin-coating, SEM, AFM, XPS

1. Introduction

Much effort has been put into improving the development and manufacture of model catalysts with well-defined metal particle sizes in the submicrometer range. Studies were published recently which introduced photolithography [1], as well as electron beam lithography [2–4], as appropriate tools for producing well-ordered arrays of nanometer-sized metal clusters. The resulting systems exhibit well-defined metal clusters with diameters as small as 30 nm on flat surfaces (usually oxidized Si wafers). The particles are easily accessible by common surface science methods, and their topography, structure and chemical composition can be examined accurately. They are very stable under high temperature and in reactive, non-oxidizing gas atmospheres. These systems were successfully tested as catalysts for hydrocarbon hydrogenation. A further method, introduced by Kuipers et al. [5], is the spin-coating of metal salt solutions onto flat substrates such as oxidized silicon wafers. The resulting salt films were then calcined and reduced to form metal clusters on the substrate. The number and size of the clusters were found to vary with the concentration of the solution, the rotational speed and the heating parameters.

Although these methods are promising, problems with the resulting systems remain to be solved. First, electron beam lithography is a very time-consuming technique, and the number of particles produced per unit time is small. Evaporation of the metals under high or ultra-high vacuum conditions is not necessarily comparable to the usual wet chemical impregnation techniques used in catalysis. On the other hand, the spin-coating method does not always lead to homogeneous systems with a narrow size distribution of the metal clusters. A small amount of dust or moisture on the substrates is, for example, sufficient to cause disordered regions with very large metal particles or leads to regions free of metal. Crucial for both techniques is that annealing the clusters in an oxidizing gas atmosphere (such as air) leads to sintering of the formerly well-ordered metal dots [2,3].

We report two methods for producing model catalyst systems. The procedures are based on the production of nanometer-sized hollows in a silicon oxide film on an entire 4 inch Si wafer. This is done by double laser interference exposure of the photoresist material covering the oxidized Si surface. Wet etching of the SiO_2 through the structured resist leads to well-ordered hollows in the flat surface of the support. Deposition of metal clusters trapped therein is achieved by evaporation as well as by spin-coating with metal salt solutions. Subsequent heating and oxidation/reduction influence the size and shape of the immobilized metal clusters. The catalysts provide sufficient metal surface area for reaction studies even at atmospheric pressure.

2. Experimental

2.1. Model catalyst preparation

2.1.1. Nanostructuring of Si(100) wafers

Silicon wafers were oxidized in a semiconductor diffusion furnace in oxygen for 2 h at 1050 °C (dry). This resulted in an oxide layer 120 nm thick. Thinned Shipley S1805 photoresist was spun on the wafers to a thickness of about 150 nm. The beam of an HeCd laser (Liconix 4270NB, 70 mW output power at 442 nm wavelength) was

* Present address: Institut für Laser- und Plasmaphysik, Uni/GH, 45177 Essen, Germany.

split and the two beams were guided to form an interference pattern on the wafers. The wafers were exposed for 4 min and rotated at 90° for a further exposition. The resist was then developed and hard baked for 0.5 h in an oven at 120 °C. The etching of the oxide layer was carried out in buffered HF (BE 50-1 from Soprelec SA) for 4 min at room temperature. The wafer was rinsed in deionised water and dried in nitrogen.

2.1.2. Deposition of metal clusters

The first method used was the evaporation of the metal on the wafers. Pd was deposited by e-gun evaporation in a Balzers BAK 550 system at an initial pressure below 1×10^{-6} mbar and at a deposition rate of 0.5 nm/s. Film thickness was controlled by a quartz microbalance. After deposition, the photoresist and, consequently, the palladium on top of the photoresist was removed ("lift-off") using Shipley remover 1165 in an ultrasonic bath for 5 min. The samples were annealed in air or under UHV conditions. The oxidized metal clusters (after annealing in air) were reduced using a high-pressure cell. Standard parameters were 1 bar pure hydrogen and a flow of 5 ml/min at 200 °C.

For the second method, the photoresist was removed without evaporation of Pd, and the structured wafers were cleaned with ethanol and acetone in an ultrasonic bath. Pieces of the wafers (1×1 cm^2) were then mounted on a commercial spin-coater, held by a vacuum chuck. Wafer fragments were used because of the size requirements of the UHV equipment and the AFM. The wafer pieces were rinsed with ethanol and acetone while rotating the sample in order to dry it and to remove dust particles from its surface. Then, about 0.05 ml of a metal salt solution (1.3 wt% $Cu(NO_3)_2 \cdot 3H_2O$ in 1-butanol as well as 1.2 wt% $Pd(CH_3COO)_2$ in cyclopentanone) was dropped onto the sample, and rotation was started after 30 s. The samples were rotated at room temperature for about 1 min. The coated samples were heated to 350 °C under UHV conditions, while the decomposition products of the inorganic compounds of the precursor materials were monitored by mass spectrometry. Furthermore, some of the samples were treated in a flow-through quartz glass reactor at atmospheric pressure in dry air at flow rates of 10–20 ml/min. Reduction of all samples took place in this quartz glass reactor in a hydrogen atmosphere at 1 bar and flow rates of 10–20 ml/min.

2.2. Analysis of model catalysts

X-ray photoelectron spectroscopy (XPS) and temperature-programmed desorption (TPD) experiments were performed in a multimethod UHV analysis chamber, described in detail elsewhere [6]. The samples (1×1 cm^2) can be transferred from a high-pressure cell (10 bar maximum working pressure) through a preparation cell (standard pressure 1×10^{-9} mbar) into the analysis chamber (standard pressure 1×10^{-10} mbar) without exposing them to atmosphere. Samples can be cooled to –180 °C and heated up to 1200 °C. XPS measurements were made using non-monochromated Al K_α radiation (1486.6 eV) at 300 W (15 kV, 20 mA).

Atomic force microscope (AFM) images were taken using a Park Scientific Instruments Autoprobe CP equipment in contact (constant force) mode and in ambient atmosphere. We used commercially available silicon cantilevers with high aspect ratio tips. Scanning electron microscopy (SEM) images were taken using a Topcon ABT-60 SEM with a video frame grabber card for direct digitizing of micrographs.

3. Results and discussion

3.1. Pitted samples with evaporated palladium inside the hollows

Figures 1 and 2 show AFM (a) and SEM (b) images of an etched wafer. All measurements shown here were done

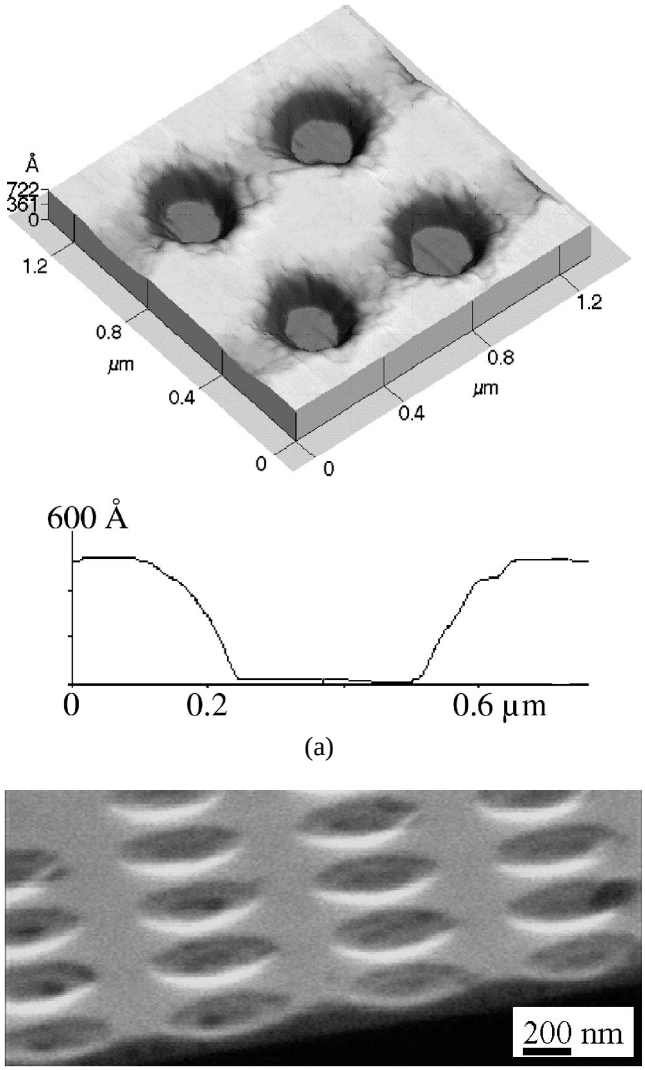

(a)

(b)

Figure 1. (a) 1.4×1.4 μm^2 AFM image of an etched silicon oxide layer after removal of the photoresist and without Pd. (b) SEM image of sample shown in (a).

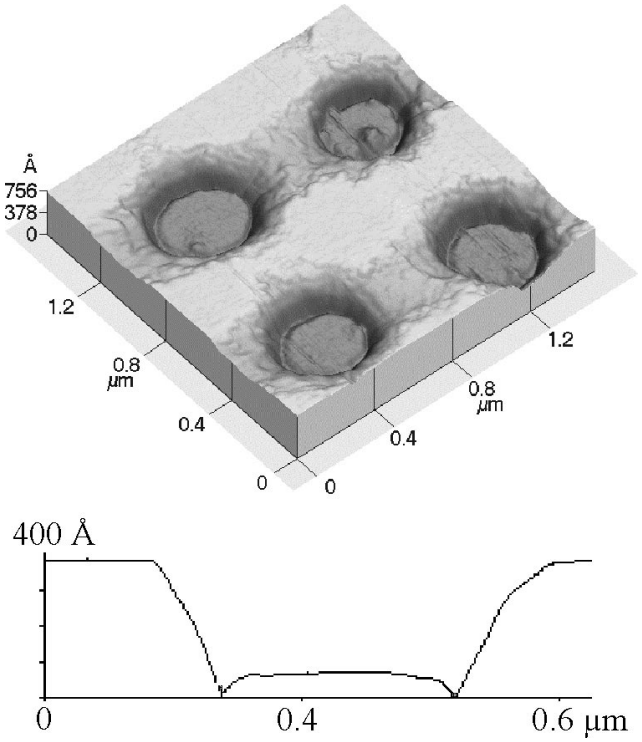

(a)

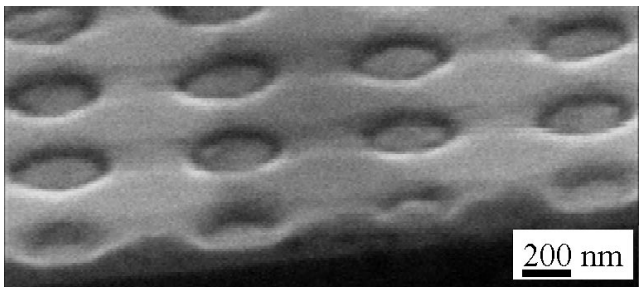

(b)

Figure 2. (a) $1.4 \times 1.4\ \mu m^2$ AFM image of an etched silicon oxide layer after removal of the photoresist and with 20 nm Pd film inside the hollows. (b) SEM image of sample shown in (a).

on the same wafer, a small region of which was covered by a piece of capton foil during metal evaporation. Images in figure 1 show the topography of the region free of palladium. The depth of the hollows is 55–60 nm. The silicon oxide was partially etched in one direction, visible as shallow grooves between the hollows. This is due to the fact that one of the laser exposures was slightly too long. In contrast to figure 1, the depth of the hollows of the sample region loaded with a 20 nm Pd film was measured to be 35 nm. Therefore, the difference in depth agrees with the thickness of the evaporated film. The flat plates, imaged at the bottom of the hollows, are surrounded by a narrow gap. These trenches around the palladium disks are due to shading effects (caused by the photoresist) during the evaporation of the metal. The shape of the hollows, as imaged, is not influenced by tip geometry, as can be seen in the SEM images of figures 1(b) and 2(b). Figure 3 shows

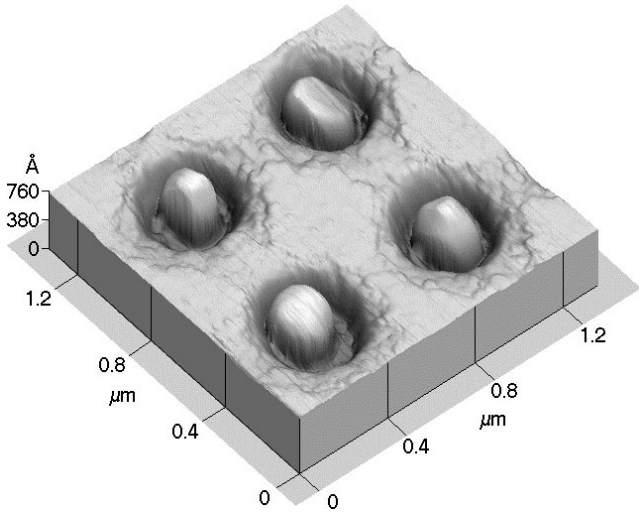

Figure 3. $1.3 \times 1.3\ \mu m^2$ AFM image of sample (as shown in figure 2(a)) after annealing to 700 °C in UHV.

the same Pd-filled sample as depicted in figure 2(a), after annealing in UHV to 700 °C. The initial heating rate was 1 °C/s. The topographic differences are clearly visible: the metal films changed their shape to isolated, hemispherical particles. Typical dimensions, as shown by the AFM, are 45 nm in height and around 200 nm in diameter. Assuming that the deposited metal films are shaped like frustums and "reconstruct" during calcination to hemispherical particles without losing material by vaporization (metal volume constant), these dimensions are reasonable values.

Figure 4 shows XPS spectra of the Pd 3d signal. The spectra were recorded at the indicated temperatures on the sample, as shown in figure 2. The heating rate was 1 °C/s. The values of binding energies given here are as measured; no charge correction was made. Binding energy was 104.5 eV for the Si 2p signal of the SiO_2, which is about 1 eV higher than usually reported for silicon oxide and typical for thick oxide films on insulating samples [7]. Heating to 300 °C leads to a slight increase in intensity (about 10%) and a slight shift in binding energy from 336.3 (341.4) to 335.9 eV (341.1 eV) of the Pd $3d_{5/2}$ ($3d_{3/2}$) signal. Both observations can be explained by the thermo-induced desorption of carbon- and oxygen-containing species from the surface (all samples were exposed to air before the examination in UHV without further cleaning, e.g., sputtering). First significant changes were found at temperatures around 500 °C. A strong decrease in intensity (integral intensity for overall intensity of Pd 3d signal, loss of more than 40% compared to the value measured at 300 °C) combined with a further shift in binding energy of 0.3 eV (from 335.9 eV at 300 °C to 335.6 eV) occurred after increasing the temperature to 500 °C. The decrease in intensity continued at even higher temperatures, as shown in the spectra recorded at 600 and 700 °C. No more shifts in binding energies were detected. The decrease in intensity is mainly caused by the changes in the structure of the particles, because in the case of the "reconstructed" particles there is less metal surface area exhibited, compared to the flat films before the

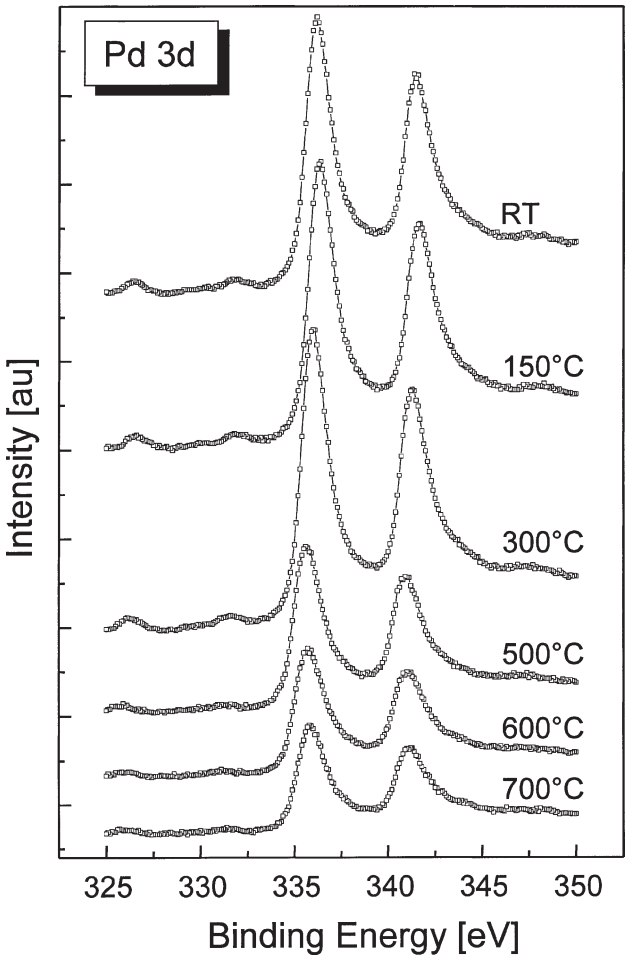

Figure 4. XPS-spectra of the Pd 3d signal of the hollowed samples evaporated with 20 nm Pd. Spectra at room temperature and at 700 °C are recorded on the sample shown in figures 2(a) and 3(a), respectively.

annealing procedure. In the case of the Pd films (as deposited), the intensity of the XPS signal is caused by a surface area of around 0.1 μm^2 per hollow (assuming an average metal film diameter of 360 nm). Once a metal disc has changed its shape and become a hemispherical particle, the complete surface area of a single hemisphere is about 60% of that value (6.2×10^{-2} μm^2, assuming an average particle diameter of 200 nm; because the reconstructed particles are not exact hemispheres but rather spheric caps, the exposed area can be even smaller than this value). The film thickness (20 nm) and the particle diameters are, in all cases, higher than the escape depth of the X-ray excited electrons. Thus, we assume that the intensity of the XPS signal is directly proportional to the exhibited palladium surface.

In full agreement with these considerations the Si 2p signal increased, while the Pd signal intensity decreased, due to the uncovering of SiO_2 inside the hollows. Loss of metal material due to bulk diffusion (e.g., alloying) or vaporization at the annealing temperatures can be more or less excluded. The calculated volumes of the metal films inside the hollows and the hemispheres after annealing are nearly constant using the above mentioned values for thickness and diameters. Thus, no metal is re-evaporated or diffused into the silicon oxide material. If this were not so then alloying of the Pd could have been detected by a shift in binding energy to higher values. This was indeed observed when using substrates with very thin oxide layers (only native oxide) at the bottom of the hollows.

Annealing the catalyst systems in air to 650 °C led to comparable results. Because of the presence of oxygen while annealing, the resulting palladium oxide particles were thereafter reduced in pure hydrogen at atmospheric pressure and hydrogen flow rates of 10 ml/min. This treat-

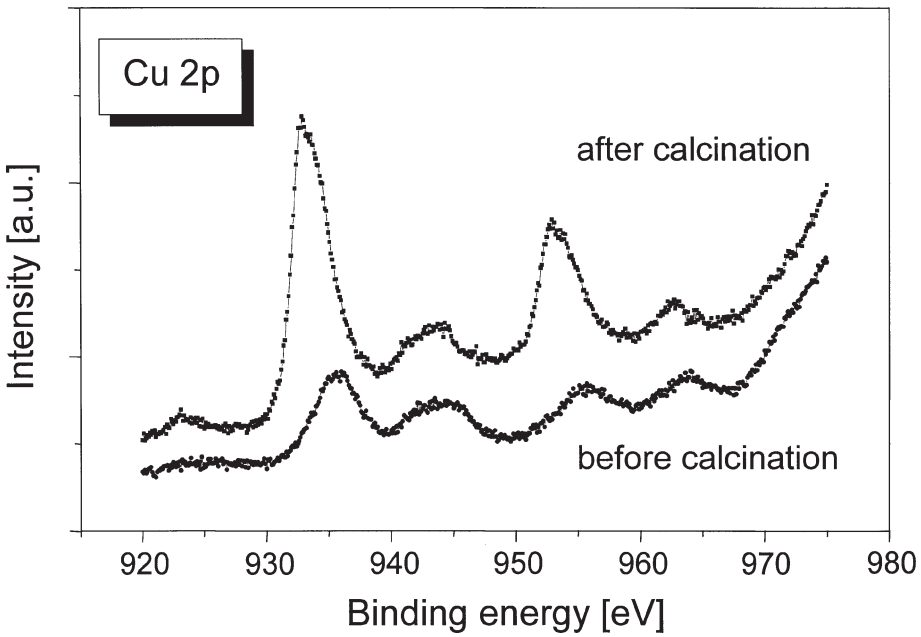

Figure 5. XPS Cu 2p signal before and after UHV annealing at 350 °C of a hollowed sample, spin-coated with $Cu(NO_3)_2 \cdot 3H_2O$ in 1-butanol.

ment did not lead to structural changes in the metal particles trapped inside the hollows.

3.2. Pitted samples and spin-coating of metal salt solutions

The number and size of the metal particles deposited by spin-coating inorganic salt solutions can be influenced by different parameters such as solution concentration and spinning speed [8,9]. However, the arrangement of the particles on the surface was affected only slightly by these parameters. Kuipers et al. reported changes in the deposition pattern on a silicon oxide surface after modifying the surface with polymeric material [10]. We used the nanostructures of the silicon oxide surface together with the spin-coating procedure to produce model catalyst systems with well-defined deposition patterns. $Cu(NO_3)_2{\cdot}3H_2O$, $Pd(CH_3COO)_2$ and $Pd(NO_3)_2$ were used as precursor materials. $Cu(NO_3)_2{\cdot}3H_2O$ was dissolved in n-butanol to give a concentration of 1.3 wt%. After coating, the samples were transferred to the UHV system, and the precursor was decomposed by heating from room temperature to 350 °C at 1 °C/s in UHV. Before and after thermo-programmed decomposition, the surface composition was measured by XPS. Figure 5 shows the increase in signal intensity and the shift in binding energy of the Cu 2p peaks after calcination. Binding energy values were 955.8 and 935.8 eV for the Cu $2p_{1/2}$ and Cu $2p_{3/2}$ lines, respectively, before calcination and 953.4 and 933.2 eV, respectively, after calcination. According to these values, the species on the surface after calcination is CuO, partially reduced after X-ray bombardment. An increase in intensity after decomposition of the precursor salt was observed in all cases investigated. Therefore, large amounts of copper ions were probably not detected, because they were shielded by the uppermost layers of the salt film on the wafer surface. The sample was then removed from the UHV chamber and transferred to the AFM. Figures 6(a) and 6(b) show topography and error signal images of the same scan, 6×6 μm^2 in size, and figure 6(c) shows a three-dimensional detail of the sample surface. It is obvious that the metal oxide clusters are, for the most part, located inside the hollows. The particle in figure 6(c) is 86 nm in diameter and 11 nm high. Although there are regions on the sample (not shown here) where no particles can be observed as well as other regions where small amounts of what is probably CuO material are located around the hollows, most of the material is deposited at the bottom of the etched features. Reduction under mild conditions (atmospheric pressure, 10 ml/min hydrogen flow, temperature below 300 °C) led to no observable topographic changes in the metal particles compared to the oxide clusters. Therefore, it is possible to produce a well-defined model catalyst system with isolated particles according to a method that is very similar to widely used catalyst impregnation methods.

The same preparation method was carried out using 1.2 wt% solutions of $Pd(NO_3)_2{\cdot}2H_2O$ in 2-pentanone and

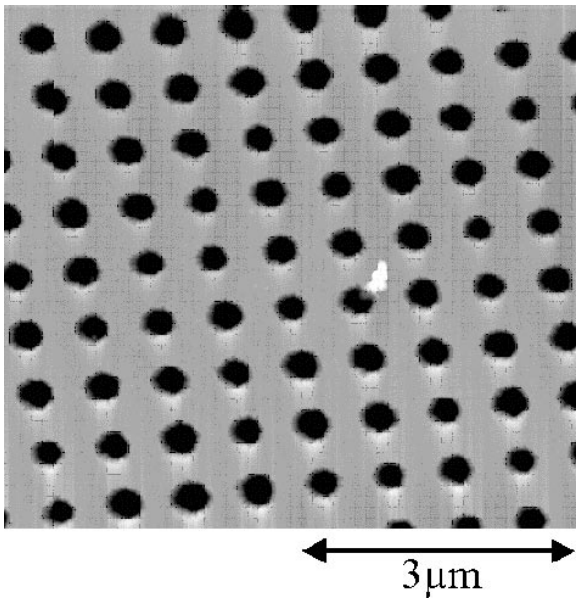

(a)

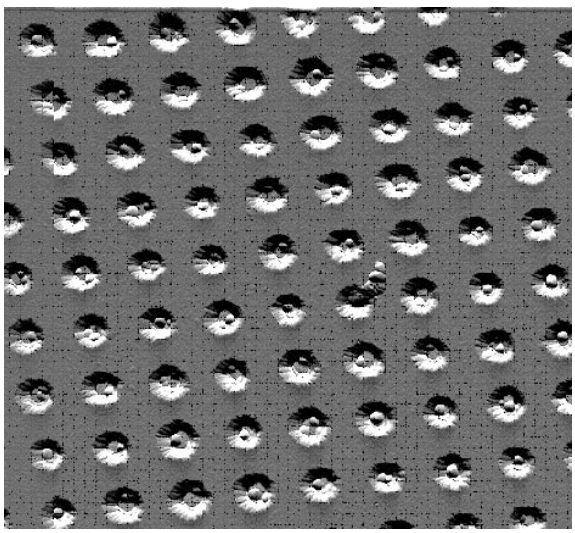

(b)

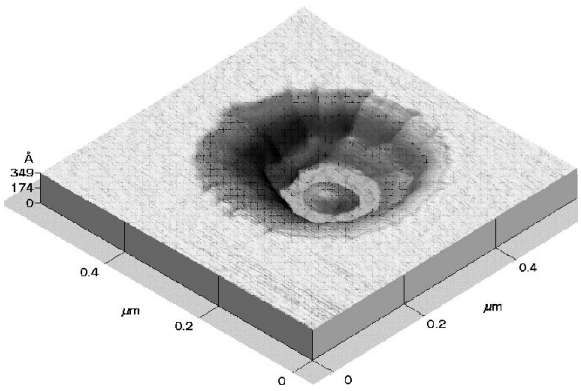

(c)

Figure 6. 6×6 μm^2 AFM images showing (a) topography and (b) error signal of a hollowed sample, spin-coated with $Cu(NO_3)_2{\cdot}3H_2O$ in 1-butanol and annealed in UHV at 350 °C. (c) is a three-dimensional detail from figure (a).

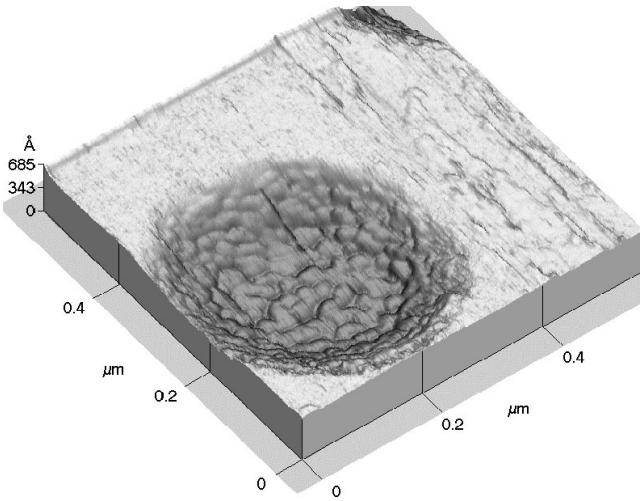

Figure 7. Three-dimensional view of a 600×600 nm^2 large AFM image of the sample spin-coated with palladium acetate in cyclopentanone after UHV annealing.

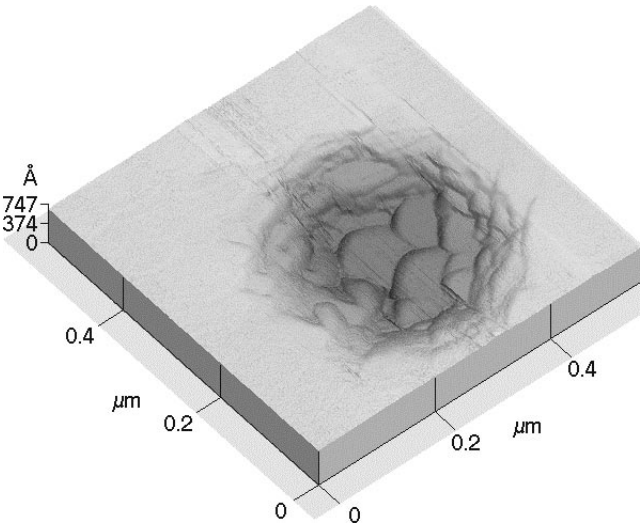

Figure 8. Three-dimensional view of a 600×600 nm^2 large AFM image. Same sample as shown in figure 7 after annealing in air (500 °C) and subsequent reduction in H_2.

$Pd(CH_3COO)_2$ in cyclopentanone. Best results were obtained using the palladium acetate solution in cyclopentanone. Figure 7 shows one hollow filled with worm-like structures of palladium oxide after annealing the sample at 300 °C in UHV. Subsequent heating in dry air at 500 °C for 1.5 h and reduction at 250 °C for 1.5 h in a flow of hydrogen led to terraced plates of the deposited material (figure 8). The terraces are around 8 nm high. Although most of the metal was again trapped inside the hollows, there was still some material left outside of the hollows in the case of Pd. This may be due to the dry air used and the applied temperature which may not have been high enough to increase the mobility of the particles on the surface. As known from investigations of small metal particles on flat substrates, sintering at elevated temperatures leads to agglomeration of the metal, mainly at steps, kinks and edges [11,12]. Thus, it is supposed that sintering of particles on the structured samples leads to agglomeration in the hollows and at their edges.

4. Conclusions

Two methods were studied for the controlled deposition of metallic particles onto a nanostructured silicon oxide surface. The evaporation of palladium through a patterned resist into pre-etched hollows as well as the wet chemical impregnation method led to perfectly ordered arrays of metal clusters with predictable sizes. The size of the clusters does not yet reach the lower nanometer region, as possible by means of electron beam lithography. However, compared to most model systems known thus far, these arrays have great potential because of the unique combination of uniformity, stability and large metal surface area (they can be produced with a large overall area on 4 inch wafers). Therefore, the catalysts provide sufficient metal surface area for reaction studies, even at atmospheric pressure. Optimizing the preparation parameters (especially reducing the thickness of the evaporated films) will help to decrease the size of the clusters. The large number of catalytically active sites as well as the mimicking of actual impregnation of such systems will help to bridge the material and pressure gaps in model catalysis.

Acknowledgement

This work is supported by a Swiss National Foundation project (NFP 36), project number 4036-044036. MS would like to thank C. Sellmer for helpful discussions.

References

[1] I. Zuburtikudis and H. Saltsburg, Science 258 (1992) 1337.
[2] M.X. Yang, D.H. Gracias, P.W. Jacobs and G.A. Somorjai, Langmuir 14 (1998) 1458.
[3] M.X. Yang, P.W. Jacobs, C. Yoon, L. Muray, E. Anderson, D. Attwood and G.A. Somorjai, Catal. Lett. 45 (1998) 5.
[4] A.C. Krauth, K.H. Lee, G.H. Bernstein and E.E. Wolf, Catal. Lett. 27 (1994) 43.
[5] E.W. Kuipers, C. Laszlo and W. Wieldraaijer, Catal. Lett. 17 (1993) 71.
[6] M. Rebholz and N. Kruse, J. Chem. Phys. 95 (1991) 7745.
[7] A. Partridge, S.L.G. Toussaint and C.F.J. Flipse, Appl. Surf. Sci. 103 (1996) 127.
[8] A. Terrasi, J. Almeida, C. Coluzza and G. Margaritondo, Nucl. Instr. Methods Phys. Res. B 116 (1996) 416.
[9] R.M. van Hardeveld, P.L.J. Gunter, L.J. van IJlzendoorn, W. Wieldraaijer, E.W. Kuipers and J.W. Niemantsverdriet, Appl. Surf. Sci. 84 (1995) 339.
[10] E.W. Kuipers, C. Doornkamp, W. Wieldraaijer and R.J. van den Berg, Chem. Mater. 5 (1993) 1367.
[11] Z.X. Chen, G.C. Smith, C.A.J. Putman and E.J.M. ter Voert, Catal. Lett. 50 (1998) 48.
[12] G. Witek, M. Noeske, G. Mestl, Sh. Shaikhutdinov and R.J. Behm, Catal. Lett. 37 (1996) 35.